Optimized EEG Channel Selection Using Power-Based Ranking and PSD Feature Modelling for EEG Signal Analysis

[1]C. Kaviyazhiny*, [2]P. Shanthi Bala, [3]S. Ajeeth, [4]R. Priyadharshini

[1, 2, 3, 4]Department of Computer Science, Pondicherry University, Pondicherry, India
[1]yazhiny02@gmail.com
[2]shanthibala.cs@gmail.com
[3]mailtoaj07@gmail.com
[4]priyadharsini.r02@gmail.com

Abstract. An electroencephalogram (EEG) is a non-invasive method used to measure brain activity and is used in various applications, such as medical, security, marketing, gaming, and brain-computer interface (BCI). EEG signals are high-dimensional and redundant in nature, which significantly complicates the channel selection process in terms of computational and analytical robustness. It is one of the critical steps in the EEG signal analysis, as the selected channels should preserve the task-relevant information without any loss. The optimal channel selection technique has been proposed using the power-based ranking and the Power Spectral Density (PSD) method. The power-based ranking method selects 9 channels from the 64 channels and extracts 9 features from the selected channels using Welch's method. Coupling features like Magnitude Squared Coherence (MAC) and Phase Amplitude Coupling (PAC) are fetched from the selected channels. Channel optimality is compared and evaluated using the spectral entropy metric, and the system achieved an average spectral entropy of 0.7234 ± 0.0216. The result shows that the proposed technique achieves high performance, reduces the system complexity, and enhances the system interoperability by reducing the number of EEG channels.

Keywords: Electroencephalogram, power-based ranking, Power spectral density, Welch's method, channel selection.

1 Introduction

EEG records non-invasive electrical brain activity, which is represented as multichannel time-series signals with stochastic amplitude variations, and it is measured in microvolts (μV). Usually, EEG signals are fluctuations in electrical potentials in the brain, measured using electrodes. These electrodes are positioned according to the international 10–20 electrode placement system. [1] [2]. This system is called the International 10-20 standard system, which is recommended by the International Federation of Societies for Electroencephalography and Clinical Neurophysiology (IFSECN). There are various regions in the brain, such as frontal, central, temporal, parietal, and occipital.

B. Singh et al. (eds.), *Proceedings of the International Conference on Advances in Computing Technology and Artificial Intelligence (COMPUTATIA 2026)*, Atlantis Highlights in Intelligent Systems 18,
https://doi.org/10.2991/978-94-6239-713-2_11

The functional activities associated with these brain regions include emotional and motor control in the frontal lobe, sensory processing in the parietal lobe, auditory perception in the temporal lobe, and visual processing in the occipital lobe. EEG electrodes are therefore labeled as FP, F, C, T, P, O, and Z to reflect their respective scalp locations. The electrode placement is from the left and from the top of the head. The left side of the lobes positions starts with the odd numbers (1,3,5,7) and the right side of the lobes positions deals with the even numbers (2,4,6,8) [3]. Auricular (A) or Mastoid (M) electrodes are commonly used as reference electrodes; therefore, they are not included in standard 10–20 scalp layout illustrations. Fig. 1 explains the 10-20 international standard system of electrode placement. Each EEG system integrates with a different number of channels as per the 10-20 international standard, but using all the channels in the system increases the system complexity and the computational cost. The selection of the minimum number of channels that contribute to the high accuracy is a vital challenge. Even though more channel usage leads to high accuracy, it has redundant EEG signals. Hence, an efficient method or technique is used for selecting the most appropriate channels from the available channels [1].

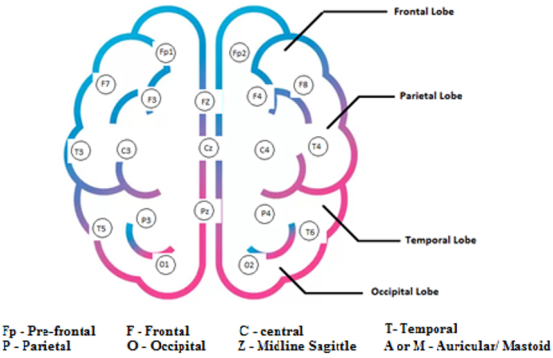

Fig. 1. 10-20 international standard system of electrode placement.

Several channel selection techniques are used that aim to choose the most informative channels by eliminating the noise and the redundancy in them. These techniques help to improve the computational efficiency, enhance the model performance, and also analyze the channels that carry the meaningful information. Depending upon the task, these algorithms are categorized into CSP-based methods, correlation-based methods, sequential-based methods, and PSO-based methods. Fig. 2. Explain the different channel selection algorithms.

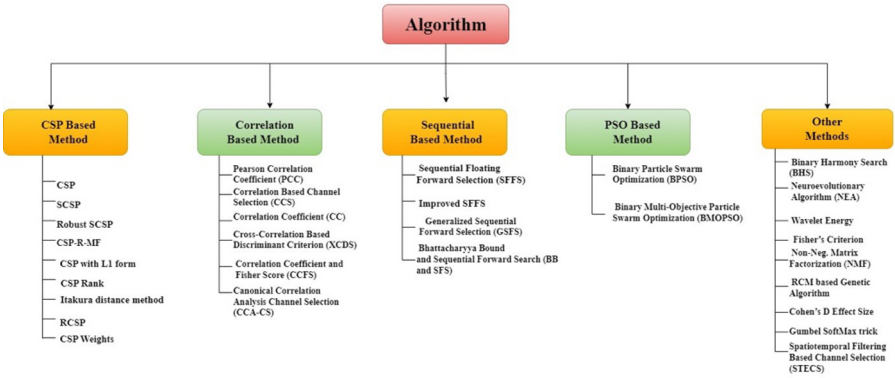

Fig. 2. Different channel selection algorithm.

The primary objective of EEG channel selection is to extract only the most relevant and informative features from a reduced set of channels, thereby minimizing computational complexity. Additionally, channel selection helps to mitigate overfitting by eliminating unnecessary channels, which improves overall performance. Furthermore, reducing the number of selected channels can significantly decrease the setup time in practical EEG-based applications [3]. The paper is organized as follows: Section 2 highlights the key findings and major trends in the literature review. Section 3 briefly discusses the methods used for optimal channel selection and the system design. Section 4 defines the experimental setup, including the dataset description. Section 5 presents the results and performance analysis of the system. Finally, Section 6 discusses the conclusions and future enhancements.

2. Related Work

In the last few decades, researchers have investigated various methods and techniques to assess the reliability of the channels in the EEG signal. [3] used a PCC-based channel selection method for selecting channels. They used the BCI competition IV dataset I, in which 14 channels were selected from 59 channels. For feature extraction and classification, Wavelet Packet Decomposition (WPD), SVM, and KNN are employed. They achieved an accuracy of 96.66% for SVM and 90.33% for KNN [3]. [4] selected 14 EEG channels from 32 channels using a Gini index–based channel ranking method. They utilized a random forest classifier for the classification, and they employed 12 features. They achieved an accuracy of 83.15 % in their model [4]. [5] selected 3 channels (Oz, T7, Cz) using the Gram-Schmidt orthogonalization reduction algorithm. They demonstrated with a deep learning technique and achieved an accuracy 98% [5]. [6] developed a single-channel EEG authentication system using DFT, DWR, and AR modelling. Entropy features were extracted, and classification was performed. They suggested O2 as the best channel and reported 97–98% accuracy, which was obtained using EEG data from seven subjects across five mental activities. They evaluated using

classifiers such as Neural Networks, Bayesian Networks, and SVM [6]. For the channel optimization, [7] demonstrated with a Face-based RSVP paradigm, Hierarchical Discriminant Component Analysis (HDCA), and Genetic Algorithm (GA), and achieved an accuracy of 94.26 % within 6 seconds [7].

[8] employed an automatic channel selection algorithm using Fisher Information and Firefly Algorithm (FA). It is a hybrid algorithm which achieved accuracy upto 83.97%. The result was examined using 3 different datasets. RCSPA was used for feature extraction, while a regularized SVM was employed for classification [8]. By integrating the mRMR, Savitzky–Golay preprocessing, and sliding windows, they implemented the Dynamic Channel Relevance (DCR) technique, which is used to select fewer channels. They employed SVM for the classification and achieved an accuracy upto 85.4% across 3 different datasets [9]. For the optimal channel selection, [15] integrated Savitzky–Golay smoothing and PCA. They achieved an accuracy of 88.80% using an XGBOOST classifier [15]. Logistic S-shaped Binary Jaya Optimization Algorithm (LS-BJOA) was demonstrated for channel selection, and it combines band pass filtering technique, ICA, and RCSP. The accuracies obtained with the classifiers are SVM (83.59) %, NB 82.09% and LDA 89.02% [10]. For channel selection, the Multiobjective X-shaped Binary Butterfly Optimization Algorithm (MX-BBOA) was employed to select a few channels. They had used an SVM classifier and obtained an accuracy of 84.49% in the BCI competition dataset [11]. Table 1 presents a comprehensive overview of the literature review.

Table 1. Review of channel selection techniques

Source	Techniques/ Algorithm	Datasets	Channels selected	Accuracy	Limitations
[3]	PCC-based channel selection, SVM/KNN classification	BCI Competition IV Dataset I	14/54	SVM: 91.66 %, KNN: 90.33 %	• PCC captures only linear relations • Only one feature (ApEn) was used • No cross-session robustness
[4]	Random Forest classifier, channel ranking via Gini Impurity	WAY_EEG_GAL	14/32	83.15 %	• Only 12 participants (small Dataset) • Only one simple motor task was tested • No cross-session stability analysis • No real-time implementation
[5]	Random Forest classifier, channel ranking	Physionet	3/64	98%	• Privacy relies on EEG fingerprinting, but security analysis is not described.

	via Gini Impurity				
[6]	DFT, DWT, AR modeling, entropy features, classifiers (Neural Network, Bayesian Network, SVM).	Keirn and Aunon	1/32	95%	• No cross-session or long-term stability analysis • Only single-channel setting tested — may limit robustness
[7]	Face-based RSVP paradigm, ERP analysis, HDCA, GA	REST	Fewer optimized channels	94.26 %	• The exact number of selected channels is not reported • Channel optimization details are not evaluated.
[8]	Fisher Information, Firefly Algorithm (FA), RCSPA, Regularized SVM	BCI Competition datasets	Fewer channels	83.97 %	• Moderate accuracy compared to deep learning methods • No analysis of long-term stability or session variability • The computational overhead of FA and RCSPA is not discussed
[9]	Dynamic Channel Relevance (DCR) using mRMR, Savitzky–Golay preprocessing, sliding windows, MEMD feature extraction, and SVM	BCI Competition datasets	Fewer channels	85.4 %	• No cross-session or long-term stability evaluation
[15]	Savitzky–Golay smoothing, FBCSP for feature extraction,	BCI Competition datasets	Not specified	88.80 %	• No real-time system evaluation or latency analysis

	PCA for dimensionality reduction, XGBoost				
[10]	LS-BJOA, Bandpass, ICA preprocessing, RCSP feature extraction, classifiers (SVM, NB, LDA).	BCI competition datasets	Fewer channels	83.59 %	• No long-term or cross-session stability evaluation
[11]	(MX-BBOA) for channel selection, Butterworth filtering, ICA artifact removal, MEMD features extraction, SVM classification	BCI competition datasets	Fewer channels	84.49 %	• The optimization overhead of MX-BBOA is not discussed

3. System Design

The proposed optimal channel selection technique uses the output from the Task Specific Dynamic Multistage K-means Clustering (TS-DMKC) algorithm [12]. The EEG signal is preprocessed using the TS-DMKC algorithm. Initially, the task-specific artifacts, such as motor movement and imagery artifacts, are separated using the Fast ICA. Then, the separated task-specific artifacts are dynamically refined using the multistage k-means algorithm. The result obtained from this stage includes a cleaned EEG signal, motor movement artifacts, and motor imagery artifacts, which are transferred to the optimal channel selection technique for the appropriate channel selection. The proposed work is the structured integration of a task-specific framework with dynamic clustering of TS-DMKC preprocessing, along with the power-based ranking and PSD feature modeling. It ensures that the selected channel preserves both spectral integrity and inter-channel functional connectivity information. Fig. 3 explains the TS-DMKC model.

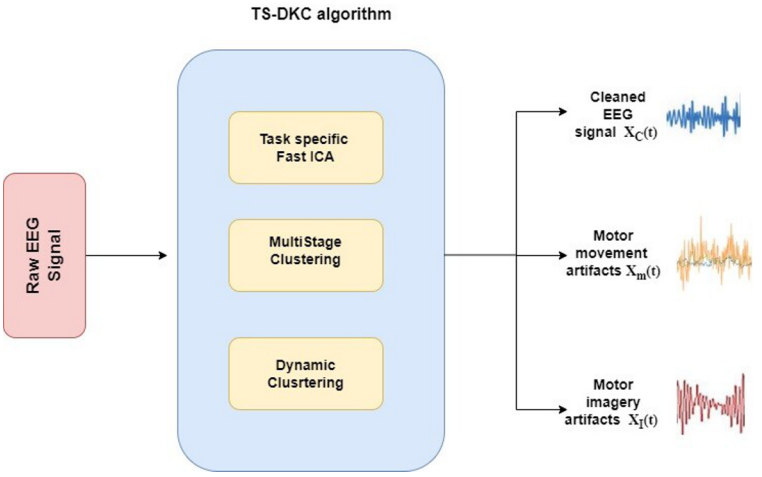

Fig. 3. TS-DMKC model

The optimal channel selection technique contains 2 stages: Power-based ranking and Multilayered feature extraction. To enhance practical deployability, the system reduces the EEG channel set to three discriminative channels. Unlike traditional fixed-electrode approaches, the proposed method uses a power-based ranking mechanism, which computes band-power significance across all channels derived from the TS-DMKC output signal. Fig. 4 elaborates on the system design.

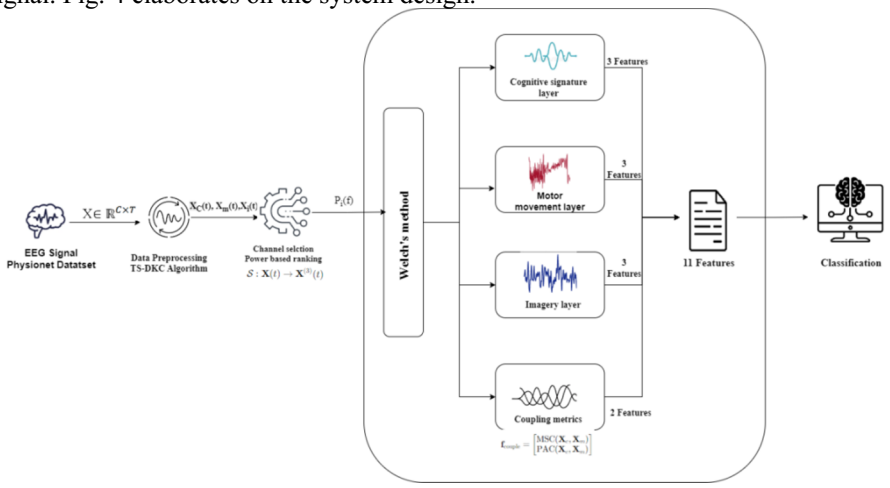

Fig. 4. Feature extractions using Welch's method.

Each output signal from the TS-DMKC is passed individually through the power-based ranking. A total of 3 channels are selected from each TS_DMKC output signals (i.e, 3 channels from cleaned EEG, 3 channels from motor movement, and 3 channels from imagery artifacts. The top three channels are selected based on spectral power, task-wise stability, and relevance to the cognitive–artifact structure identified by TS-DMKC.

This step significantly reduces system complexity while retaining discriminative neural information and also fetches the best features from the signals. The power-based ranking is calculated using the formula (1). Given the EEG signal X∈R^(C×T) , c is the number of channels, T is the number of time samples, and Pi is the total signal power of that channel across all time samples [12]. The signal power of channel i is computed using equation (1):

$$P_i = \sum_{t=1}^{T} X_i\,(t)^2$$

Where Xi(t) is the signal amplitude of channel i at time t.

In stage 2, Multilayered feature extraction contains four layers, such as the Cognitive signature layer, Motor movement layer, Motor imagery layer, and Coupling layer. The three selected channels from Stage 1 are processed through three distinct layers: cognitive signature, motor movement, and motor imagery. In all layers, features are extracted using Power Spectral Density (PSD) via the Welch's method, which includes log-transformed band power to stabilize inter-trial variations, as computed in equation (2) [13]. Given a signal Xi(t), Welch's method estimates the PSD by dividing the signal into overlapping segments, applying a window, and averaging the periodograms of each segment. Let Xi(t) be the EEG signal, L be the segment length, D be the overlap between segments, K be the number of segments, w[n] be the window function, U be the window normalization or scaling factor, k be the index, and Xk(m) be the DFT of the k-th windowed segment.

The Welch's PSD P_i (f). The estimate for channel i is calculated using equation (2),

$$P_i(f) = \frac{1}{KU}\sum_{k=1}^{K} \left| \sum_{n=0}^{L-1} X_i[n + kD]w[n]e^{-\frac{j2\pi fn}{L}} \right|$$

where

$$U = \frac{1}{L}\sum_{n=0}^{L-1} w[n]^2$$

3.1 Cognitive signature layer

The cleaned EEG signal is computed in this layer using Welch's method, and the log-based power is extracted as a feature. The extracted features summarize canonical EEG frequency bands and dominant spectral patterns. The extracted features reflect steady-state cognitive rhythms, which are both user-specific and temporally stable.

3.2 Motor movement layer

In the traditional method, the extracted artifacts are removed and discarded as noise, but in the proposed system, they are repurposed as biometric features. The motor movement layer computes motor artifacts using Welch's method and extracts three log-band power features representing neuromotor activation patterns. These features encode involuntary muscular and physiological traits that complement cognitive features.

3.3 Motor imagery layer

Motor imagery produces cortical activation patterns distinct from both cognitive signals and physical movement artifacts. These patterns are subtle but consistent across sessions for an individual. The imagery layer generates three imagery-specific features representing imagined movement dynamics. Combining imagery with movement and cognitive layers yields richer biometric features.

3.4 Coupling layer

In Beyond isolated features, the system analyzes interactions between cognitive and artifact components. Magnitude-Squared Coherence (MSC) and Phase Amplitude Coupling (PAC) are the two coupling metrics that are computed in this layer. Frequency-domain synchrony between cognitive and artifact layers is captured by MSC, which reflects the brain–body interaction stability. Cross-frequency interaction between phases of motor artifacts and amplitude of cognitive signals is captured by PAC, which gives a higher-order biomarker of coordinated neural modulation. These metrics uniquely quantify how cognitive and artifact processes are relatively unexplored, but they provide highly distinctive information that can effectively differentiate individuals in an EEG-based system. A unified multidimensional EEG signature vector is formed by concatenating all these extracted features (3 cognitive + 3 movement + 3 imagery + 2 coupling = 11 features). The concatenation of these feature groups yields the final multidimensional EEG signature, which serves as the input to the downstream classification module in future studies. This unified representation is subsequently employed for user identification and verification, allowing the system to discriminate between individuals based on their characteristic neural and artifact-coupled patterns.

4. Experimental Setup and Dataset

The experimental setup utilized a Windows 11 Pro workstation equipped with an AMD Ryzen 5 5600X 6-core processor and configured with an NVIDIA RTX A4000 GPU featuring 16,375 MiB of dedicated VRAM, which utilized CUDA version 11.7 for GPU-accelerated computations. The Dataset used in the proposed work is "The EEG Motor Movement/Imagery Dataset" offered by Physionet, which consists of 64-channel EEG recordings from 109 subjects performing motor and motor imagery tasks. Each subject in the Dataset performs 14 experimental sessions, which include 2 baseline recordings (eyes open and eyes closed) and 12 task sessions involving motor execution and motor imagery tasks [12]. Table 2 discusses the experimental configurations

Table 2: Experimental Configuration

Component	Specifications
Sampling Rate	160 Hz
PSD Method	Welch
Window Length	256 samples

Overlap	50%
Cognitive Band	1-50 Hz
Motor Band	30-50 Hz
Imagery Band	4 -12 Hz
Coupling Features	MSC (1), PAC (1)
Sampling Rate	160 Hz
Feature Distribution	3 Cognitive, 3 Motor, 3 Imagery, 2 Coupling
Total Features	11 (fixed across sessions)

5. System Analysis

The proposed optimal channel selection method is implemented and evaluated using the Physionet dataset. From the clean EEG signal, motor movement and imagery artifacts, nine channels have been selected. To ensure robustness and consistency of the proposed technique, the channels were identified across fourteen sessions. The variation in selected channels across the 14 sessions provides the adaptive and session-specific behaviour of our channel ranking strategy rather than instability. Since EEG signals are inherently non-stationary and subject-dependent [14], the proposed model dynamically selects the most discriminative channels per session to preserve task-relevant information. Despite channel variability, performance metrics remain consistent, demonstrating the robustness and reproducibility of the proposed channel selection model. Table 3 details the 9 channels selected from 14 different sessions, which highlights the stability and relevance of the selected channels for future analysis.

Table 3. Selected channels across 14 sessions

Sessions	Selected channels		
	Cleaned EEG Signal	Motor movement	Motor imagery
Session 1	Fp1, Fp2, Af7	Cp5, Cp3, C5	Cp6, Fc6,C6
Session 2	Po8,O1,O2	C5,Fc4,C4	Tp7,T9,T7
Session 3	Fp1,Fp2,Af7	P7, T7,P5	C2,Cp4,Cp2
Session 4	Fp1,Af7,Fp2'	T7,C3,Cp4	F8,F6,Ft7.
Session 5	Fp1,Fp2,Af8	Tp8,T8,Cp2	Po8,Ft7,Po4
Session 6	Fp1,'Fp2,Af7	T8,Iz,F6	Po8,P6,P8
Session 7	Fp1,Fp2,Af7	F8, C2,Fc6	Fc5,C5,Ft7
Session 8	Fp1,Af7,Af3	Fc6,'Fc5,P5	Po8,P6,Cp6
Session 9	Fp1,Fp2,Fpz	'P7,P5,Tp7	Cp2,Cp4,Cp6
Session 10	Fp1,Fp2,Af7	T7,P7,Tp7	C4,Fc4,P4
Session 11	Fp1,Fp2,Af7	T8,C2,Cp2	Cp5,F6,P6
Session 12	Fp1,Af7,Af3	F8,Ft7,Tp7	P4,Cp4,C4
Session 13	Fp1,Fp2,Af7	Po8,Cp3,Po4	P7P5,Tp7

Spectral entropy is used as the primary metric, as it's suitable for channel selection evaluation. It measures the information richness and spectral complexity, which is a key indicator of neural signal integrity. The calculation of spectral entropy has been

done among the nine selected channels across 14 sessions. In which the selected nine channels exhibited lower spectral entropy values. This indicates the more structured and informative neural activity. The non-selected channels exhibit higher spectral values, which indicate increased randomness in the EEG signal and reduced discriminative relevance. The mean spectral value achieved across the 14 sessions is 0.7467, and the overall mean spectral entropy value achieved by the proposed method was 0.7234 ± 0.0216, which indicates the effectiveness of the proposed channel selection approach in preserving informative neural structures.

For the comparative analysis, configurations with 2, 3, and 5 EEG channels were evaluated to determine the optimal channel selection. The average spectral entropy values for the 2-channel, 3-channel, and 5-channel configurations were 0.7480, 0.7467, and 0.7989, respectively. The 3-channel configuration exhibits less spectral entropy, comparable to that of the 2-channel setup, while providing a richer feature representation due to the increased number of feature vectors. In contrast, the 5-channel configuration shows substantially higher spectral entropy, indicating increased signal complexity and redundancy. These results demonstrate that the 3-channel selection achieves the best balance between information richness and signal complexity, and it is identified as the most suitable choice among the evaluated configurations. Variations in spectral entropy across the 2, 3, and 5 channel configurations are noticed, as evaluation selects the highest log-based (dB) features, which reflect both spectral entropy fluctuation and potential redundancy. Table 4 presents the comparative analysis of spectral entropy across 14 sessions. The statistical analysis is conducted to evaluate whether there is a significant difference in spectral entropy between selected and non-selected EEG channels across sessions using a two-way repeated measures ANOVA. The analysis assumes normal distribution of spectral entropy values, sphericity of repeated measures, and independence of observations, with significance evaluated at $\alpha = 0.05$.

Null Hypothesis (H_0): There is no significant difference in spectral entropy between selected and non-selected channels across sessions.
Alternate Hypothesis (H_1): There is a significant difference in spectral entropy between selected and non-selected channels across sessions.
If the p-value is less than 0.05, the null hypothesis (H_0) is rejected; otherwise, it is accepted. In this study, the ANOVA results show a significant main effect of channel type ($F(1,13) = 91.96$, $p < 0.001$). Since the obtained p-value is less than the significance threshold, the null hypothesis (H_0) is rejected. This indicates that there is a statistically significant difference in spectral entropy between selected and non-selected channels across sessions, confirming the effectiveness of the proposed channel selection approach.

Table 4. Comparative analysis of spectral entropy

Sessions	2 Channel selection		3 Channel selection		5 Channel selection	
	Selected channels (6 Channels)	Non-selected (58 channels)	Selected channels (9 Channels)	Non-selected (55 channels)	Selected channels (15 Channels)	Non-selected (49 channels)

Session 1	0.7468	0.7549	0.7452	0.7556	0.7406	0.7583
Session 2	0.7788	0.7989	0.7971	0.7970	0.7878	0.7999
Session 3	0.7313	0.7667	0.7360	0.7679	0.7287	0.7740
Session 4	0.7836	0.7853	0.7761	0.7867	0.7669	0.7908
Session 5	0.7417	0.7719	0.7462	0.7729	0.7450	0.7765
Session 6	0.7163	0.7586	0.7198	0.7603	0.7253	0.7636
Session 7	0.7297	0.7624	0.7312	0.7639	0.7333	0.7673
Session 8	0.7483	0.7802	0.7512	0.7815	0.7561	0.7837
Session 9	0.7500	0.7855	0.7434	0.7886	0.7513	0.7917
Session 10	0.7234	0.7771	0.7443	0.7766	0.7387	0.7823
Session 11	0.7416	0.7434	0.7199	0.7471	0.7138	0.7522
Session 12	0.7233	0.7624	0.7316	0.7632	0.7250	0.7691
Session 13	0.7337	0.7756	0.7479	0.7756	0.7458	0.7796
Session 14	0.7673	0.7828	0.7635	0.7843	0.7584	0.7884

Fig. 5 elaborates on the 11 features selected from 9 channels and the 2 coupling metrics. The feature set comprises cognitive, motor, and motor imagery representations, each captured through three feature components, in addition to Magnitude-Squared Coherence (MSC) and Phase–Amplitude Coupling (PAC) measures that model inter-channel and cross-frequency interactions. Cognitive features show the highest and most stable spectral entropy, which indicates dominant and reliable neural information. Imagery features have a moderate entropy value, while motor features are lower, reflecting progressively more structured activity. The figure highlights clear separability and consistency among the feature groups across recording sessions, demonstrating the effectiveness of the proposed feature selection strategy.

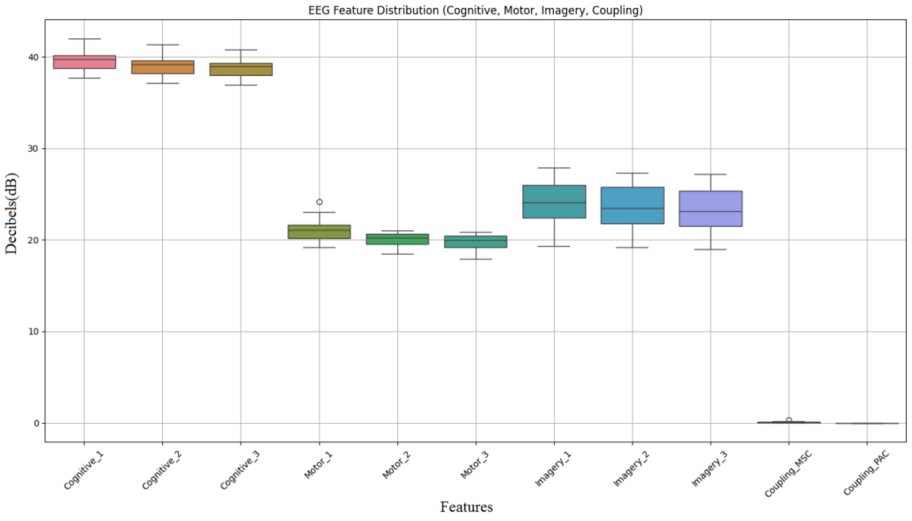

Fig. 5: Extracted 11 features

6. Conclusion

The proposed channel selection techniques can effectively support efficient EEG signal processing by preserving informative neural patterns. The channels are selected using channel-based ranking, and the features are extracted using the Welch's method (PSD) and coupling metrics. The evaluation of the proposed technique was carried out using the Physionet motor movement/imagery dataset. It demonstrates strong reliability, robustness, and applicability across various EEG applications and achieved a low spectral entropy of 0.7234 ± 0.0216, indicating the preservation of highly informative neural structures. For the performance evaluation, a comprehensive set of eleven features, encompassing cognitive, motor movement, motor imagery, and coupling representations, is employed, which effectively captures both spectral and interaction-based neural characteristics. The proposed work may be extended to real-time and cross-subject EEG applications by incorporating adaptive, learning-based channel selection and attention-driven fusion models to enhance discriminative performance.

References

1. The T. Alotaiby, F. E. A. El-Samie, S. A. Alshebeili, and I. Ahmad, "A review of channel selection algorithms for EEG signal processing," EURASIP Journal on Advances in Signal Processing, vol 1, pp. 66, 2015.
2. C. Kaviyazhiny, P. S. Bala, R. Priyadhrashini, and S. Ajeeth, "Analysis of Factors Impacting the Efficiency of EEG-Based Biometric Authentication System", International Conference on System, Computation, Automation and Networking (ICSCAN), pp. 1-7, 2024.
3. R. Dhiman, "Electroencephalogram channel selection based on pearson correlation coefficient for motor imagery-brain-computer interface," Measurement: Sensors, vol. 25, pp. 100616, 2023.
4. E. C. Ketola, M. Barankovich, S. Schuckers, A. Ray-Dowling, D. Hou, and M. H. Imtiaz, "Channel reduction for an EEG-based authentication system while performing motor movements," Sensors, vol. 22(23), pp. 9156, 2022.
5. A. J. Bidgoly, H. J. Bidgoly, and Z. Arezoumand, "Towards a universal and privacy preserving EEG-based authentication system," Scientific Reports, vol. 12(1), pp. 2531, 2022.
6. M. Zeynali and H. Seyedarabi, "EEG-based single-channel authentication systems with optimum electrode placement for different mental activities," Biomedical Journal, vol. 42(4), pp. 261-267, 2019.
7. Y. Zeng, Q. Wu, K. Yang, L. Tong, B. Yan, J. Shu, and D. Yao, "EEG-based identity authentication framework using face rapid serial visual presentation with optimized channels," Sensors, vol. 19(1), pp. 6, 2018.
8. A. Tiwari and A. Chaturvedi, "Automatic EEG channel selection for multiclass brain-computer interface classification using multiobjective improved firefly algorithm," Multimedia Tools and Applications, vol. 82(4), pp. 5405-5433, 2023.
9. A. Tiwari and A. Chaturvedi, "A novel channel selection method for BCI classification using dynamic channel relevance," IEEE Access, vol. 9, pp. 126698-126716, 2021.

10. A. Tiwari, "A logistic binary Jaya optimization-based channel selection scheme for motor-imagery classification in brain-computer interface," Expert Systems with Applications, vol. 223, pp. 119921, 2023.
11. A. Tiwari and A. Chaturvedi, "Automatic channel selection using multiobjective X-shaped binary butterfly algorithm for motor imagery classification," Expert Systems with Applications, vol. 206, pp. 117757, 2022.
12. C. Kaviyazhiny, P. S. Bala, R. Priyadharshini, and S. Ajeeth, "Task-Specific Electroencephlogram Analysis: A Novel ICA and Dynamic Multistage Clustering Approach for Neural Signal Processing," International Journal of Imaging Systems and Technology, vol. 36(1), pp. e70260, 2026.
13. J. G. Proakis, Digital signal processing: principles, algorithms, and applications, 4th ed., Pearson Education India, 2007.
14. W. Klonowski, "Everything you wanted to ask about EEG but were afraid to get the right answer," Nonlinear Biomedical Physics, vol. 3, no. 1, pp. 2, 2009.
15. A. Tiwari and A. Chaturvedi, "A Multiclass EEG Signal Classification Model using Spatial Feature Extraction and XGBoost Algorithm," 2019 IEEE/RSJ International Conference on Intelligent Robots and Systems (IROS), pp. 4169-4175, 2019.